

W.W.Hansen Experimental Physics Laboratory
STANFORD UNIVERSITY
STANFORD, CALIFORNIA 94305-4085

Gravity Probe B Relativity Science Mission

ON THE LINEARITY OF GRAVITY PROBE B
MEASUREMENT MODEL

S0632, Rev.A

May, 2003

Prepared by:


I. Mandel, Research Assistant

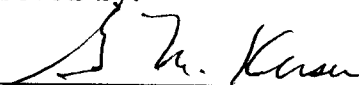
05/30/03
Date

Prepared by:


A. S. Silbergleit, Senior Research Scientist


05/30/03
Date

Approved by:


G. M. Keiser, Chief Scientist

6/17/03
Date

ITAR Assessment Performed


(Tom Langenstein)

ITAR Control Req? Yes

No

6.17.03

1 Introduction

Magnetic dipole, which is developed, according to F. London, by a rotating superconductor, is always aligned with its rotation axis. The Gravity Probe B London moment readout is provided by measuring the London dipole magnetic flux through the pick-up loop of the SQUID [1]. Hence the readout signal is proportional to the sine of the angle (say, β_{LM}) between the gyro spin axis and the plane of the pick-up loop. The angle is rather small, thus, as shown in [2], its cube can be safely neglected for the required experimental accuracy, and the readout proves thus to be linear in this angle.

To detect relativistic drift of the gyro spin axis relative to the inertial reference of the Guide Star (GS), we need to use a proper model expression for β_{LM} as a function of time. It is desired to be as simple as possible while meeting, at the same time, the accuracy requirements. For this reason, the formula for β_{LM} is usually simplified by neglecting higher powers of certain other small angles involved, such as, for instance, the angle between the apparent and true directions to the GS, or the spin to roll axis misalignment.

The validity of such assumptions, which has never been systematically studied before, is examined in the next section of this document. It is demonstrated that in the answer there are, in fact, no terms quadratic in those small angles. Therefore the first corrections to the linear terms turn out to be cubic, and thus small enough to be safely neglected, so that the linear measurement equation can be retained.

Another potential source of nonlinear terms in the measurement equation for the SQUID signal is some nonlinearity of electronic circuits and devices through which the signal runs onboard (see c. f. [1]). The effects of these nonlinearities on the measurement error is studied in sections 3 and 4. The results are summarized in section 5.

2 Linearity of London Moment Readout: Expression for the Angle Between Gyro Spin Axis and Pick-Up Loop Plane

Let $\hat{\tau}$ be the unit vector in the apparent direction to the GS where the telescope is pointing, and which is also the direction of the satellite roll axis. Let \hat{x} and \hat{y} be the unit vectors fixed in the body of the satellite, such that $(\hat{x}, \hat{y}, \hat{\tau})$ form a right-handed Cartesian basis.

In the inertially fixed frame defined by the GS Cartesian basis $(\hat{e}_{NS}, \hat{e}_{EW}, \hat{e}_{GS})$ [3], the vector $\hat{\tau}$ is given by

$$\hat{\tau} = \tau_{NS}\hat{e}_{NS} + \tau_{EW}\hat{e}_{EW} + \sqrt{1 - \tau_{NS}^2 - \tau_{EW}^2}\hat{e}_{GS}, \quad (1)$$

where τ_{NS} is the sum of the aberration, starlight bending, parallax, telescope pointing error and perhaps some other optical effects [1, 3, 4], projected onto the NS direction, and similarly for τ_{EW} . Note that, in fact, τ_{NS} and τ_{EW} are functions of time changing slowly as compared to the roll period. Also, Gravity Probe B operates in the regime with $|\tau_{NS}|, |\tau_{EW}| \ll 1$, that is, the telescope is pointing very close to the true direction to the GS.

Let us denote the satellite angular velocity by ω_r . This is the velocity of rotation around the $\hat{\tau}$ axis. To describe this rotation, we write down the expressions for the unit vectors \hat{x}_0 and \hat{y}_0 forming a Cartesian right-handed basis together with $\hat{\tau}$. Apparently, there is some freedom in their choice represented by an arbitrary initial phase, or, equivalently, by an arbitrary start time. So we pick a phase that allows \hat{x}_0 to have no component in the \hat{e}_{EW} direction, i.e., for which

$$\hat{x}_0 = x_{0NS} \hat{e}_{NS} + x_{0GS} \hat{e}_{GS}.$$

Then, from the conditions $\hat{x}_0 \cdot \hat{\tau} = 0$ and $\hat{x}_0 \cdot \hat{x}_0 = 1$, we obtain

$$\hat{x}_0 = -\frac{\sqrt{1 - \tau_{NS}^2 - \tau_{EW}^2}}{\sqrt{1 - \tau_{EW}^2}} \hat{e}_{NS} + \frac{\tau_{NS}}{\sqrt{1 - \tau_{EW}^2}} \hat{e}_{GS}.$$

Now \hat{y}_0 should be defined as

$$\hat{y}_0 = \frac{\hat{\tau} \times \hat{x}_0}{|\hat{\tau} \times \hat{x}_0|} = \frac{\tau_{EW}\tau_{NS}}{\sqrt{1 - \tau_{EW}^2}} \hat{e}_{NS} - \sqrt{1 - \tau_{EW}^2} \hat{e}_{EW} + \frac{\tau_{EW}\sqrt{1 - \tau_{NS}^2 - \tau_{EW}^2}}{\sqrt{1 - \tau_{EW}^2}} \hat{e}_{GS}.$$

The vectors $\hat{x}(t)$ and $\hat{y}(t)$ can be derived from \hat{x}_0 and \hat{y}_0 by means of the standard Euler rotation matrix, giving

$$\begin{aligned} \hat{x}(t) = & \cos \omega_r t \hat{x}_0 + \sin \omega_r t \hat{y}_0 = \\ & \frac{1}{\sqrt{1 - \tau_{EW}^2}} \left[\left(-\sqrt{1 - \tau_{NS}^2 - \tau_{EW}^2} \cos \omega_r t + \tau_{EW}\tau_{NS} \sin \omega_r t \right) \hat{e}_{NS} - \right. \\ & \left. \left(1 - \tau_{EW}^2 \right) \sin \omega_r t \hat{e}_{EW} + \right. \\ & \left. \left(\tau_{NS} \cos \omega_r t + \tau_{EW}\sqrt{1 - \tau_{NS}^2 - \tau_{EW}^2} \sin \omega_r t \right) \hat{e}_{GS} \right] \end{aligned} \quad (2)$$

and

$$\begin{aligned} \hat{y}(t) = & -\sin \omega_r t \hat{x}_0 + \cos \omega_r t \hat{y}_0 = \\ & \frac{1}{\sqrt{1 - \tau_{EW}^2}} \left[\left(\sqrt{1 - \tau_{NS}^2 - \tau_{EW}^2} \sin \omega_r t + \tau_{EW}\tau_{NS} \cos \omega_r t \right) \hat{e}_{NS} - \right. \\ & \left. \left(1 - \tau_{EW}^2 \right) \cos \omega_r t \hat{e}_{EW} + \right. \\ & \left. \left(-\tau_{NS} \sin \omega_r t + \tau_{EW}\sqrt{1 - \tau_{NS}^2 - \tau_{EW}^2} \cos \omega_r t \right) \hat{e}_{GS} \right]. \end{aligned} \quad (3)$$

The SQUID pick-up loop makes an angle α ($\ll 1$) with the satellite roll axis $\hat{\tau}$. Therefore, in the $\hat{x}, \hat{y}, \hat{\tau}$ body-fixed system, the normal unit vector to the pick-up loop plane can be written in the form

$$\hat{n} = \sqrt{1 - \alpha^2} \cos \phi_0 \hat{x} + \sqrt{1 - \alpha^2} \sin \phi_0 \hat{y} + \alpha \hat{\tau}, \quad (4)$$

where ϕ_0 is some constant phase.

We can now substitute the expressions for \hat{x} , \hat{y} and $\hat{\tau}$ from equations (2), (3), and (1) into the equation (4) to obtain \hat{n} in the inertially-fixed frame of the GS, namely

$$\begin{aligned}
\hat{n} = & \left[\frac{\sqrt{1-\alpha^2} \cos \phi_0}{\sqrt{1-\tau_{EW}^2}} \left(-\sqrt{1-\tau_{NS}^2-\tau_{EW}^2} \cos \omega_r t + \tau_{EW} \tau_{NS} \sin \omega_r t \right) + \right. \\
& \frac{\sqrt{1-\alpha^2} \sin \phi_0}{\sqrt{1-\tau_{EW}^2}} \left(\sqrt{1-\tau_{NS}^2-\tau_{EW}^2} \sin \omega_r t + \tau_{EW} \tau_{NS} \cos \omega_r t \right) + \\
& \left. \alpha \tau_{NS} \right] e_{\hat{NS}} + \left[-\sqrt{1-\alpha^2} \cos \phi_0 (1-\tau_{EW}^2) \sin \omega_r t - \right. \\
& \left. \sqrt{1-\alpha^2} \sin \phi_0 (1-\tau_{EW}^2) \cos \omega_r t + \alpha \tau_{EW} \right] e_{\hat{EW}} + \\
& \left[\sqrt{1-\alpha^2} \cos \phi_0 \left(\tau_{NS} \cos \omega_r t + \tau_{EW} \sqrt{1-\tau_{NS}^2-\tau_{EW}^2} \sin \omega_r t \right) + \right. \\
& \left. \sqrt{1-\alpha^2} \sin \phi_0 \left(-\tau_{NS} \sin \omega_r t + \tau_{EW} \sqrt{1-\tau_{NS}^2-\tau_{EW}^2} \cos \omega_r t \right) + \right. \\
& \left. \alpha \sqrt{1-\tau_{NS}^2-\tau_{EW}^2} \right] e_{\hat{GS}}
\end{aligned} \tag{5}$$

Next, let \hat{s} denote the direction of the spin axis (London moment) of the gyroscope. In the inertial GS frame the unit vector \hat{s} can be written as

$$\hat{s} = NS \hat{e}_{NS} + EW \hat{e}_{EW} + \sqrt{1-(NS)^2-(EW)^2} \hat{e}_{GS}. \tag{6}$$

Here the current North-South misalignment NS is the sum of the initial misalignment NS_0 , relativistic drift, and the drift due to classical torques, and similarly for East-West misalignment EW . Under the GP-B conditions, both misalignments are small, $|NS|, |EW| \sim 10^{-4}$ at most.

Finally, the angle β_{LM} between the London moment direction, \hat{s} , and the pick-up loop plane is given by

$$\beta_{LM} \approx \sin \beta_{LM} = \hat{s} \cdot \hat{n} \tag{7}$$

By working in the inertial basis, we can easily compute this dot product. We write it down to the second order in the small quantities $\tau_{NS}, \tau_{EW}, NS, EW, \alpha$:

$$\begin{aligned}
\beta_{LM} = & -NS \cos \omega_r t \cos \phi_0 + NS \sin \omega_r t \sin \phi_0 - \\
& EW \sin \omega_r t \cos \phi_0 - EW \cos \omega_r t \sin \phi_0 + \\
& \tau_{NS} \cos \omega_r t \cos \phi_0 + \tau_{EW} \sin \omega_r t \cos \phi_0 - \\
& \tau_{NS} \sin \omega_r t \sin \phi_0 + \tau_{EW} \cos \omega_r t \sin \phi_0 + \\
& \alpha + \text{cubic terms in all the angles} .
\end{aligned}$$

Trivial trigonometric grouping of terms allows us to obtain the final expression for β in a compact form:

$$\beta = (\tau_{NS} - NS) \cos(\omega_r t + \phi_0) + (\tau_{EW} - EW) \sin(\omega_r t + \phi_0) + \alpha + \text{cubic terms} + \dots \quad (8)$$

The coefficients in front of the roll harmonics are just the differences of the current gyroscope and telescope misalignments (caused, respectively, by mechanical and optical factors) in the two directions perpendicular to the true direction to the GS. Thus, we recovered our first order signal model [1, 5], and demonstrated that all corrections to it are cubic in the small angles. At worst, the corrections should be not larger in the order than 10^{-13} , which is definitely negligible as compared to the order $10^{-5} - 10^{-4}$ of the main linear terms.

3 Electronic Nonlinearities of SQUID Readout

There are several sources of readout nonlinearities in the onboard electronics. The SQUID itself is an intrinsically nonlinear device. Namely, although the magnetic flux in the SQUID, Φ_s , is directly proportional [6] to the flux in the pick-up loop, Φ :

$$\Phi_s = \Phi/363, \quad (9)$$

the output voltage of the SQUID, V_{SQ} , is a nonlinear function of Φ_s , well approximated by a cubic polynomial:

$$V_{SQ} = C_{SQ} \Phi_s \left(1 + 10^{-4} \Phi_s + 5 \times 10^{-5} \Phi_s^2 \right), \quad (10)$$

where C_{SQ} is the proper scale factor. Note that the small coefficients on the right are the result of the optimization of the operational point of the SQUID. Note also that both Φ and Φ_s are *dimensionless*, expressed by the number of magnetic flux quanta, Φ_0 ; in particular,

$$\Phi = \Phi_{in}/\Phi_0, \quad (11)$$

where Φ_{in} is the dimensional flux in the loop.

Let us show that the nonlinearity (10) can be neglected, for the required GP-B accuracy of one part in a hundred thousands. For this, we express the dimensionless flux in the loop through the equivalent London moment angle, β_L , by the formula (see [2], (I.1.3)):

$$\Phi = \frac{\Phi_{LM}}{\Phi_0} = \frac{2\pi N_* M_L}{R} \frac{2e}{\hbar c} \beta_L = 8\pi^2 N_* \frac{r}{R} \frac{m_e r^2 f_s}{h} \beta_L. \quad (12)$$

Here R is the pick-up loop radius, $N_* = 4$ is the effective number of turns of the pick-up loop [6], M_L is the dipole magnetic London moment whose expression is used in the utmost right, r is the rotor radius, m_e and h are the mass of electron and the Plank constant, respectively, and f_s is gyro spin frequency. After substituting the proper values of all the parameters involved, we obtain

$$\Phi = c_L \beta_L, \quad c_L = 40 N_* f_s = 160 f_s, \quad (13)$$

where the value of spin frequency should be taken in Hz . The SQUID range in terms of the equivalent London moment angle is $\beta_L^{max} = 100 \text{ as} = 4.85 \times 10^{-4} \text{ rad}$; a plausible spin speed of the GP-B gyro is $f_s = 150 \text{ Hz}$. Therefore, by (9) and (13),

$$\max \Phi_s = \max \Phi / 363 = 160 \times 150 \times 4.85 \times 10^{-4} / 363 = 0.032. \quad (14)$$

Accordingly, the nonlinearity in (10) is at most 3.2×10^{-6} , and we can definitely neglect it.

Thus, the output readout voltage after passing the whole onboard electronic circuit, including the A/D converter, can be generally written in terms of the flux in the pick-up loop as [see (11)]:

$$V_{out} = C\Phi_{in} \left[1 + \epsilon_2 \left(\frac{\Phi_{in}}{\Phi_{max}} \right) + \epsilon_3 \left(\frac{\Phi_{in}}{\Phi_{max}} \right)^2 + \dots \right] + b = \\ (C\Phi_0)\Phi \left[1 + \epsilon_2 (\Phi_0/\Phi_{max}) \Phi + \epsilon_3 (\Phi_0/\Phi_{max})^2 \Phi^2 + \dots \right] + b, \quad (15)$$

where C and b are the readout scale factor and bias, respectively. The harmonic distortions $\epsilon_2, \epsilon_3, \dots$ are constant in the low frequency range $f \sim 1 \text{ mHz} - 1 \text{ Hz}$, which we only discuss here. The typical for GP-B magnitudes of the first two harmonic distortions are [7]:

$$\epsilon_2 = 3.7 \times 10^{-4}, \quad \epsilon_3 = 9.4 \times 10^{-4}. \quad (16)$$

It is more convenient for us to study the effects of nonlinearity in terms of the equivalent London moment angle, β_L , rather than the dimensionless magnetic flux, Φ . So, we substitute the expression (13) for the latter through the former in the formula (15). Using the equality

$$c_L \Phi_0 / \Phi_{max} = 1 / \beta_L^{max},$$

implied by (13) and (11), we find:

$$V_{out} = C_g \beta_L \left[1 + \epsilon_2 (\beta_L / \beta_L^{max}) + \epsilon_3 (\beta_L / \beta_L^{max})^2 + \dots \right] + b, \quad (17)$$

or

$$C_g \beta_L (1 + a_2 \beta_L + a_3 \beta_L^2 + \dots) + b. \quad (18)$$

The new scale factor, C_g , is related to the old one, C , by

$$C_g = c_L \Phi_0 C = 160 f_s \Phi_0 C, \quad (19)$$

and the magnitudes of the new harmonic distortion coefficients, a_2, a_3, \dots , are:

$$|a_2| = |\epsilon_2| / \beta_L^{max} = 0.75, \quad |a_3| = |\epsilon_3| / (\beta_L^{max})^2 = 4000, \dots \quad (20)$$

Since the higher order harmonics were found to be much stronger suppressed in the GP-B readout signal, we limit ourselves with only the quadratic and cubic nonlinearities in the analysis below.

4 Effects of Electronic Nonlinearity

4.1 Overall Nonlinear Effect on the Readout

The basic measurement model used for GP-B data reduction does not contain any terms nonlinear in β_L . So, for the validity of the linear measurement model it would be best if the total relative nonlinear corrections were less than 10^{-5} . As seen from (17) and (16), this requires, however, $\beta_L/\beta_L^{max} < 0.1$, which is never true if, for instance, the calibration signal (see the next section) is present. At $\beta_L/\beta_L^{max} = 0.5$, which is about a peak number for the GP-B signal, the relative contribution of nonlinearity is about 3×10^{-4} . Therefore it would seem that the accurate analysis of the SQUID readout requires modeling of nonlinearities. Fortunately, this turns out not completely correct because of the specific structure (time signature) of the signal, which we are going to consider in detail.

4.2 Time Signature of the Low Frequency SQUID Signal

We now introduce the time dependence of all the low frequency components of the equivalent London moment angle $\beta_L = \beta_L(t)$ [recall that, by (13), the dimensionless flux in the pick-up loop is $\Phi = c_L \beta_L$]. In the presence of the London moment signal, trapped flux, and calibration signal, taking also into account the intrinsic SQUID bias, it can be written as a sum of the four respective contributions:

$$\beta_L(t) = \beta_{LM}(t) + \beta_T(t) + \beta_c(t) + \beta_b(t). \quad (21)$$

Let us examine each of the contributions.

According to (8), the London moment angle, $\beta_{LM}(t)$, is

$$\begin{aligned} \beta_{LM}(t) &= A_{LM} \cos \phi_r(t) + \alpha, \\ A_{LM} &= \sqrt{(\tau_{NS} - NS)^2 + (\tau_{EW} - EW)^2}, \quad \phi_r = \omega_r t + \phi_{r0}, \end{aligned} \quad (22)$$

[see also [2], formula (I.2.10); note that only the low frequency components are included]. The slowly varying amplitude of the roll harmonics is $A_{LM} < 30 as = 1.5 \times 10^{-4}$. This maximum value consists of $20.5 as = \sqrt{5^2 + 20^2} as$ of orbital and annual aberrations taken at their peaks, with almost $10 as$ left for the spin-to-roll misalignment, which, in fact, is required to be within just $1 as$ averaged over the year of observations. Hence, this is the worst-on-worst upper bound, which, most probably, will never be reached during the experiment. Also, $\alpha = 55 as = 2.7 \times 10^{-4}$ is a constant angle between the roll axis and pick-up loop plane involved in (4).

The trapped flux contribution, $\beta_T(t)$, turns out to be

$$\beta_T(t) = (c_T/c_L) \beta_{LM}(t) = (c_T/c_L) [A_{LM} \cos \phi_r(t) + \alpha], \quad (23)$$

where c_T is the flux-to-angle coefficient for the low frequency trapped flux in the pick-up loop [see [2], formula (II.2.16); note once again that we include only the low frequency components]. Generally it is a periodic function of time with the polhode period; its magnitude could be very conservatively estimated as $|c_T/c_L| \leq 0.05$.

The angle $\beta_c(t)$ represents the calibration signal,

$$\beta_c(t) = A_c \cos \phi_c(t) \quad \phi_c = \omega_c t + \phi_{c0} . \quad (24)$$

A very stable (to one part in 10^5) calibration signal amplitude A_c will be kept within $30 \text{ as} = 1.5 \times 10^{-4}$.

Finally, the magnitude of the equivalent SQUID bias angle, $\beta_b(t)$, is determined by the threshold of the bias offset algorithm, whose reasonable value is 5 as . Within this threshold, the long-term variations, such as the thermal ones, are estimated to be extremely low, below 1 mas , so they can be safely neglected. On the other hand, the big fast jumps in the bias, caused by energetic cosmic particles at a rate of about one hit per day, will be immediately countered by the bias reset algorithm. Therefore in our analysis we can consider the bias angle constant,

$$\beta_b(t) = \beta_b = \text{const} = 2.5 \times 10^{-5} ; \quad (25)$$

the effect of changing this constant abruptly, i. e., of the bias reset, on the scale factor is studied in section 4.6.

Summing up the expressions (23), (23), (24), and (25), we write the equivalent London angle (21) in a convenient form:

$$\beta_L(t) = A_r \cos \phi_r(t) + A_c \cos \phi_c(t) + A_T ; \quad (26)$$

$$A_r = (1 + c_T/c_L) \sqrt{(\tau_{NS} - NS)^2 + (\tau_{EW} - EW)^2}, \quad A_T \equiv (1 + c_T/c_L) \alpha + \beta_b . \quad (27)$$

For the estimates that follow, and that are not sensitive to the time variation, we will use the worst case values

$$A_r = A_c = 1.5 \times 10^{-4}, \quad A_T = 3 \times 10^{-4}, \quad (28)$$

according to the above discussion and the formula (27). On the other hand, wherever necessary, the time variation of A_r and A_T will be taken into account using

$$A_r = 1.5 \times 10^{-4} [1 + \varepsilon u(t)], \quad A_T = 3 \times 10^{-4} [1 + \varepsilon u(t)], \quad \varepsilon = 0.05, \quad (29)$$

where the function $|u(t)| < 1$ describes the polhode modulation.

The calibration signal frequency can have just two fixed values, $1/62 \text{ Hz}$ and $1/124 \text{ Hz}$. The roll frequency during the data acquisition period is expected to be $1/180 \text{ Hz}$. In any case, the two frequencies will be well separated, and their combination frequencies, with much smaller amplitudes, will not influence the GP-B signal enclosed in the slow variation of the amplitude at roll. For this reason, when introducing (26) into (18) to get the SQUID output voltage in terms of various harmonics, we retain only the multiple harmonics of the roll and calibration frequencies. In this fashion, we obtain:

$$V_{out} = C_g \left\{ \sum_{n=1}^3 [A_r^{(n)} \cos(n\phi_r) + A_c^{(n)} \cos(n\phi_c)] + \dots \right\} + B, \quad (30)$$

where the constant C_g is given in (19), the dots stand for the dropped harmonics we are not interested in,

$$B = b + C_g [A_T(1 + a_2 A_T + a_3 A_T^2) + 0.5(a_2 + 3a_3 A_T)(A_r^2 + A_c^2)], \quad (31)$$

and

$$A_r^{(1)} = A_r \left[1 + 2a_2 A_T + 0.75 a_3 \left(A_r^2 + 2 A_c^2 + 4 A_T^2 \right) \right] ; \quad (32)$$

$$A_r^{(2)} = 0.5 A_r^2 (a_2 + 3a_3 A_T); \quad (33)$$

$$A_r^{(3)} = 0.25 a_3 A_r^3 . \quad (34)$$

Evidently, the amplitudes of the calibration signal harmonics are given by the same formulas in which the indices r and c replace each other:

$$A_c^{(1)} = A_c \left[1 + 2a_2 A_T + 0.75 a_3 \left(A_c^2 + 2 A_r^2 + 4 A_T^2 \right) \right] ; \quad (35)$$

$$A_c^{(2)} = 0.5 A_c^2 (a_2 + 3a_3 A_T); \quad (36)$$

$$A_c^{(3)} = 0.25 a_3 A_c^3 . \quad (37)$$

These are the desired expressions allowing one to analyze the main effects of the nonlinearity on the SQUID readout.

4.3 Harmonic Distortion at Roll and Calibration Frequencies

Formulas (33), (36), and (20) provide the same estimate for the relative amplitudes of the second harmonics of both roll and calibration frequencies:

$$\frac{A_i^{(2)}}{A_i} = 0.5 A_i (a_2 + 3a_3 A_T) < 8.4 \times 10^{-5}, \quad i = r, c . \quad (38)$$

For the third harmonics, from (34), (37), and (20) one finds:

$$\frac{A_i^{(3)}}{A_i} = 0.25 a_3 A_i^2 < 7.3 \times 10^{-5}, \quad i = r, c . \quad (39)$$

The above estimates do not imply that one necessarily needs to model higher harmonics in the GP-B data analysis. Indeed, those are the worst-on-worst case estimates, since the calibration signal amplitude could be deliberately reduced 2–3 times, and the typical value of the roll signal amplitude is at least two times smaller than the one used. Most importantly, if not modeled, higher harmonics would just add somewhat to the noise whose influence on the accuracy of the relativistic drift determination is strongly reduced by the large number of measurements. However, the check for higher harmonics of the roll and calibration frequencies should be perhaps carried out periodically during the experiment.

4.4 Time Variation in Scale Factors of the Science and Calibration Signals Caused by Nonlinearity

The scale factor of the science signal, i. e., the scale factor at the roll frequency, $C_g(\omega_r)$, is defined in a natural way as

$$V_{out}(\omega_r) = C_g(\omega_r) A_r .$$

The accuracy of the relativistic drift measurement requires, within the baseline data analysis, that $C_g(\omega_r)$ is constant to one part in 10^5 , which issue is examined here.

According to the equations (30) and (32), the scale factor at roll is given by the expression:

$$C_g(\omega_r) = C_g \left[1 + 2a_2 A_T + 0.75 a_3 \left(A_r^2 + 2 A_c^2 + 4 A_T^2 \right) \right]. \quad (40)$$

The effect of the nonlinearity on the scale factor at roll is described thus by

$$\begin{aligned} \frac{\delta C_g(\omega_r)}{C_g} &\equiv \frac{C_g(\omega_r) - C_g}{C_g} = 2a_2 A_T + 0.75 a_3 \left(A_r^2 + 2 A_c^2 + 4 A_T^2 \right) = \\ &1.5 A_T + 3000 \left(A_r^2 + 2 A_c^2 + 4 A_T^2 \right). \end{aligned} \quad (41)$$

Any additions to unity on the utmost right of (41) do not play any role as soon as they stay constant, i. e., do not change with the time. Their variable part is obtained from introducing expressions (29) for A_r and A_T in (41), which, to lowest order in the modulation parameter $\varepsilon = 0.05$, provides the variation of the scale factor at roll in the form

$$\left| \frac{\delta C_g(\omega_r)}{C_g} \right|_{var} = 1.39 \times 10^{-4} |u(t)| < 1.4 \times 10^{-4}. \quad (42)$$

This worst-on-worst number is about an order of magnitude larger than the desired one. It is proportional to the level of the polhode modulation set at 5% in our estimate. Most probably, the actual level of modulation will be just about 1%; combined with a two times reduction of the typical amplitude at roll, this gives an acceptable value of the time variation in the scale factor. Nevertheless, additional measures should be taken to further reduce this variation, and modeling of the polhode modulation of the scale factor in the GP-B data analysis may be needed.

As implied by (35), the scale factor at the calibration frequency is

$$C_g(\omega_c) = V_{out}(\omega_c)/A_c = C_g \left[1 + 2a_2 A_T + 0.75 a_3 \left(A_c^2 + 2 A_r^2 + 4 A_T^2 \right) \right]. \quad (43)$$

Its properties are also very important, since we check on the scale factor at roll by measuring it. The effect of the nonlinearity on $C_g(\omega_r)$, by (43), is:

$$\begin{aligned} \frac{\delta C_g(\omega_c)}{C_g} &\equiv \frac{C_g(\omega_c) - C_g}{C_g} = 2a_2 A_T + 0.75 a_3 \left(A_c^2 + 2 A_r^2 + 4 A_T^2 \right) = \\ &1.5 A_T + 300 \left(A_c^2 + 2 A_r^2 + 4 A_T^2 \right). \end{aligned} \quad (44)$$

Because of the twice larger coefficient in front of A_r^2 here as compared to (41), the variable part turns out slightly larger than in the case of roll:

$$\left| \frac{\delta C_g(\omega_c)}{C_g} \right|_{var} = 1.45 \times 10^{-4} |u(t)| < 1.5 \times 10^{-4}. \quad (45)$$

An important feature of the time variation in both scale factors is that the source of it, i. e., the trapped flux polhoding, and thus its time signature, are the same in both cases.

4.5 Ratio of Scale Factors of the Science and Calibration Signals

For the reason stated above, it is also useful to look at the ratio of the scale factors,

$$\frac{C_g(\omega_r)}{C_g(\omega_c)} = \frac{1 + 2a_2 A_T + 0.75 a_3 (A_r^2 + 2 A_c^2 + 4 A_T^2)}{1 + 2a_2 A_T + 0.75 a_3 (A_c^2 + 2 A_r^2 + 4 A_T^2)} = 1 - \frac{3000 (A_r^2 - A_c^2)}{1 + 1.5 A_T + 3000 (A_c^2 + 2 A_r^2 + 4 A_T^2)} . \quad (46)$$

Dropping higher order terms, which are smaller than 10^{-9} , we obtain

$$\frac{C_g(\omega_r)}{C_g(\omega_c)} \approx 1 - \delta, \quad |\delta| = 3000 |A_r^2 - A_c^2| < 7.75 \times 10^{-5}, \quad (47)$$

in the worst-on-worst case.

4.6 Effect of the SQUID Bias Reset on the Scale Factor

A SQUID bias reset, i. e., an abrupt change in β_b value from (25) for our analysis means, according to (27), the replacement of A_T with some $A_T + \delta A_T$. As seen from (41) and (44), it leads to the same change in both the roll and calibration signal scale factors,

$$\left| \frac{\delta C_g(\omega_i)}{C_g} \right|_{reset} = (2a_2 + 6 a_3 A_T) \delta A_T + 3a_3 (\delta A_T)^2 = (1.5 + 24000 A_T) \delta A_T + 900 (\delta A_T)^2, \quad i = r, c . \quad (48)$$

The last quadratic term on the right is completely negligible even for the biggest resets having $\delta A_T = 30 \text{ as}$. For the resets with $\delta A_T = 1 \text{ as}$, expression (48) gives

$$\left| \frac{\delta C_g(\omega_i)}{C_g} \right|_{reset} = 4.2 \times 10^{-5}, \quad (49)$$

which rate tentatively shows that many bias resets should not inflict significant changes on the scale factor.

5 Conclusions

Here is a brief summary of our results.

1. Geometrical nonlinear corrections to the model (8) of the angle between the London moment and pick-up loop plane used in GP-B data reduction are at least eight orders of magnitude smaller than the main linear term.
2. Contributions of the intrinsic SQUID nonlinearity (10) is, in the worst case, about one order of magnitude smaller than required by the experiment accuracy.
3. The estimates of the effect of the onboard electronics nonlinearity that follow deal only with the quadratic and cubic nonlinearities. The analysis is carried out for the low frequency SQUID signal consisting of the London moment, trapped flux, and calibration signals in the presence of a constant intrinsic SQUID bias.
4. The worst-on-worst case second harmonic distortion is within 8.4×10^{-5} for both the science and calibration signals. The corresponding limit on the third harmonic distortion is 7.3×10^{-5} .

5. The ratio of the scale factors of the science and calibration signals differs from unity by less than 7.8×10^{-5} in the worst-on-worst case.
6. The worst-on-worst case time variation in both the science and calibration signal scale factors, due to bias changes, is about 10^{-4} of the magnitude. The plausible value for the science scale factor variation is estimated to be within 2×10^{-5} .
7. The worst-on-worst case relative change in both the science and calibration signal scale factors, due to SQUID bias reset, is 4.2×10^{-5} per 1 *as* of the bias change.

References

- [1] G.M.Keiser, A.S.Silbergleit, M.I.Heifetz. *Gravity Probe B Data Analysis*. GP-B doc. S0597, Stanford University, 2001.
- [2] G.M.Keiser, A.S.Silbergleit. *Pick-Up Loop Symmetry and Centering*. GP-B doc. S0243, Stanford University, 1995.
- [3] M.I.Heifetz, A.S.Krechetov, A.S.Silbergleit. *Model of Starlight deflection and Parallax for GP-B Data Reduction*. GP-B doc. S0393, Stanford University, 2001.
- [4] A.S.Silbergleit. *Observable Effects and Measurement Model*. Science Advisory Committee Meeting-5, January 4-5, 2001. GP-B, HEPL, Stanford University, 2001.
- [5] G.M.Keiser, M.I.Heifetz, A.S.Silbergleit, A.S.Krechetov, I.V.Mandel. *Gravity Probe B Data Reduction and Simulation Algorithms. End-to-End Test #3: Summary*. GP-B doc. S0434, Stanford University, 2000.
- [6] G.M.Keiser, J.Lockhart, B.Muhlfelder. *Bias Variation in the Gravity Probe B Gyroscope Readout System*. GP-B doc. S0352, Stanford University, 2003.
- [7] G.M.Keiser. *Verification of T002 Requirement 5a*. GP-B doc. S0868, Stanford University, 2003.